Iranian Journal of Materials Forming 11 (2) (2024) 75-95

Online ISSN: 2383-0042

Iranian Journal of Materials Forming

Journal Homepage: http://ijmf.shirazu.ac.ir

Review Article

Investigating the Effect of Ultrasonic Shot Peening Parameters on Metallurgical, Mechanical, and Corrosion Properties of Industrial Parts: A Literature Review

A. Omidi Hashjin[1], M. Vahdati[1*] and R. Abedini[2]

[1] Faculty of Mechanical Engineering, Shahrood University of Technology, Shahrood, Iran
[2] Department of Mechanical Engineering, Iran University of Science and Technology, Tehran, Iran

ARTICLE INFO

Article history:

Received 30 April 2024
Reviewed 30 July 2024
Revised 3 August 2024
Accepted 8 August 2024

Keywords:

Ultrasonic shot peening
Surface treatment
Compressive residual stress
Corrosion resistance

Please cite this article as:

Omidi Hashjin, A., Vahdati, M., & Abedini, R. (2024). Investigating the effect of ultrasonic shot peening parameters on metallurgical, mechanical, and corrosion properties of industrial parts: A literature review. *Iranian Journal of Materials Forming*, *11*(2), 75-95. https://doi.org/10.22099/ijmf.2024.50081.1294

ABSTRACT

Ultrasonic shot peening (USP) is a surface treatment technique widely employed in the automotive, aerospace, and marine industries to enhance the mechanical and metallurgical properties of components. This enhancement is achieved by inducing compressive residual stresses on material surface using spherical shots resonated by a vibrating body, known as the sonotrode. The controllability of USP, with variables such as shot properties (material and size), peening distance, peening duration, peening intensity, peening coverage, and the amplitude of sonotrode vibration, has attracted significant attention from engineers and researchers. To ensure the industrial reliability of USP, a thorough investigation of the process is necessary. This paper aims to review relevant research conducted since 1999 to shed light on the effects of USP on different material properties, including grain size, fatigue strength, corrosion behavior, hardness, and other mechanical, metallurgical, and electrochemical characteristics. A review of the pertinent literature demonstrates that USP can effectively reduce surface grains of materials to a range of 10 to 100 nm while producing surface compressive residual stresses up to 900 MPa. It also significantly enhances fatigue resistance at low strain amplitudes by retarding crack initiation and growth. Although USP increases surface roughness, it can improve corrosion resistance when applied with an optimal peening duration. Additionally, USP can substantially increase hardness, yield strength, tensile strength, and wear resistance.

1. Introduction

According to DIN 8200, peening involves a mechanical method for hardening the surface of materials. This process utilizes the peening media of a particular shape and material, which are activated within various peening devices. This media then interacts with the surface of the workpiece [1]. Shot peening is a process that impacts the surface of materials with spherical balls, hence producing a compressive residual stress (CRS) layer on the surface of the material. As a result, the impacts from the shot peening process lead to plastic deformations, thereby causing alterations in the material surface

* Corresponding author
E-mail address: vahdati@shahroodut.ac.ir (M. Vahdati)
https://doi.org/10.22099/ijmf.2024.50081.1294

properties [2]. As depicted in Fig. 1, shot peening can be implemented through various systems, including rotating wheel, compressed-air, injector, and injector gravitational setups. These systems are differentiated by their specific methods for accelerating the spherical shots [1].

Intensity is a major parameter of the shot peening process. John Almen observed that shot peening caused the exposed surface of sheet metals to stretch and bend. In response, he devised the Almen strip as a means to gauge the compressive stresses induced in the metal by the shot peening process. Almen also established a standardized procedure to measure the kinematic energy imparted to the material surface by using the shot stream. This energy is commonly referred to as the intensity at saturation in shot peening specifications. Measurement of the peening intensity is achieved by assessing its impact on standardized Almen strips, using a specialized tool called the Almen gauge. Almen's method for measuring the peening intensity has been widely embraced and incorporated into the engineers' design processes. The following components are necessary for determining the peening intensity according to the Almen method [2]:

- Almen test strips
- Almen gage
- Test strip holding fixture (Almen holder)

Three types of Almen strips are specified, consisting of standard test strips made from spring steel SAE1070 tempered to 44-50 HRC. These strips vary in thickness for use at different intensity levels. Fig. 2 demonstrates the procedure for measuring peening intensity using the aforementioned tools. After the strip is exposed to the shot stream and removed from the holding fixture, the gage stem is positioned against the untreated surface. The measured strip deflection indicates a single arc height corresponding to the exposure time [2].

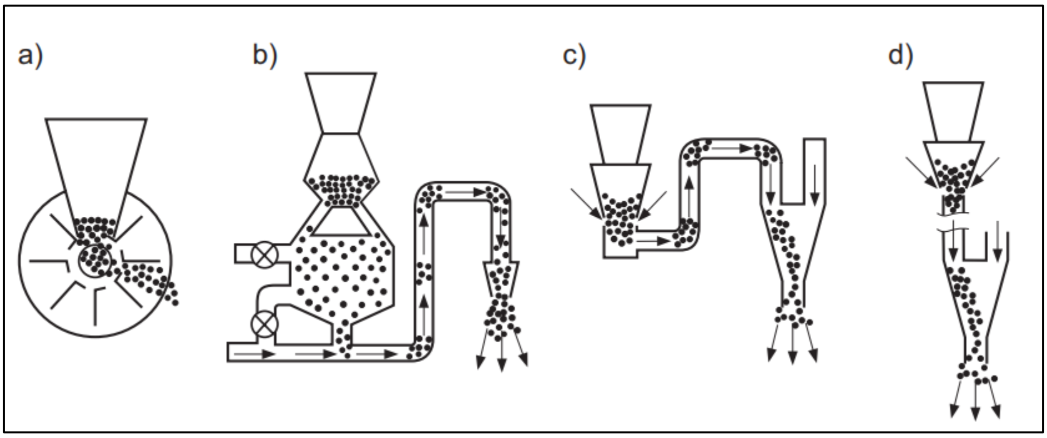

Fig. 1. Different methods of shot peening implementation: (a) rotating wheel, (b) compressed air, (c) injector and (d) injector gravitational peening devices [1].

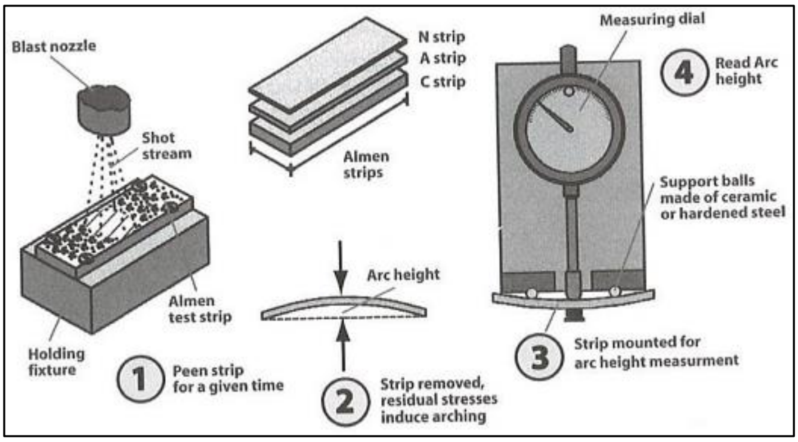

Fig. 2. Schematic of the Almen method and tools for measuring the peening intensity [2].

Intensity is defined as the arc height of a shot-peened test strip at its saturation point. The saturation point refers to the earliest point on the saturation curve where if the exposure time is doubled, the arc height increases by 10% or less. To determine peening intensity, it's essential to establish a saturation curve, achieved by peening a series of Almen strips with different exposure times while keeping all other peening parameters constant. By plotting the arc height deflection of these strips against exposure time, a curve similar to that shown in Fig. 3 is achieved. The saturation time (T) is identified as the earliest point on this curve where doubling the exposure time (2T) results in no more than a 10% increase in the arc height. The Almen intensity corresponds to the specific arc height obtained at the saturation time [2].

Another important parameter in shot peening is surface coverage, which represents the percentage of the surface that has been impacted at least once and affected by the shot blast stream, taking into account the angle of the stream relative to the workpiece surface [2].

Ultrasonic shot peening (USP) differs from conventional shot peening (CSP) by the way the impact media is excited. Instead of relying on constant air flow, gravity, or the high-speed rotation of a turbine, USP employs acceleration of a vibrating body known as the sonotrode. The frequency of the vibration of the sonotrode falls within the ultrasonic wave range, typically between 18 and 20 kHz [3]. Schematic of USP process and its main components are illustrated in Fig. 4. According to Fig. 4, the transducer converts the electrical signals produced by the ultrasonic generator into low-amplitude reciprocating motions, which are boosted by the amplitude transformer and then transmitted to the shots through the sonotrode. Consequently, the shots gain kinetic energy and begin to impact the surface of the workpiece multiple times in a short period due to their stochastic motion, in an enclosure called the peening chamber, leading to the formation of surface CRS. The main controllable USP parameters are:

- Shot material
- Shot size (diameter)
- Number of shots
- Workpiece material
- Peening distance: the distance between the surface of the workpiece and the face of the sonotrode
- Peening duration
- Peening coverage
- Sonotrode amplitude of vibration
- Peening intensity

2. Literature Review

One of the most effective ways to understand how a strain hardening process affects materials and to determine its industrial efficiency and reliability is to review relevant research conducted over the years. This paper reviews the pertinent research conducted on USP process from 1999 to 2024. The studies conducted during the mentioned period could be categorized into the following topics:

- Surface nanocrystallization and generation of compressive residual stresses
- Impact of USP on fatigue properties
- Influence of USP on surface characteristics, mechanical properties, corrosion behavior, and microstructure of materials

Therefore, to enhance clarity and comprehensibility, the literature review is divided into the aforementioned subsections. This division provides a comprehensive understanding of the effects of the USP process on material properties.

2.1. Surface nanocrystallization and generation of compressive residual stresses

Materials featuring nanograins have demonstrated superior properties compared to those with standard grain size [4]. This implies that the average grain size of a material plays a significant role in determining its strength, as reflected in the well-known Hall-Petch relation [5]:

$$\sigma_y = \sigma_0 + kd^{-1/2} \quad (1)$$

In the Hall-Petch relation, σ_y represents the yield strength of the refined-grain material, σ_0 denotes the initial yield strength of the material, *d* stands for the average grain size, and *k* is the yielding constant. As per this relation, when the average grain size decreases, the yield strength increases [5].

As previously stated, the primary goal of USP is to induce formation of CRS, which in turn results in surface grain refinement, also referred to as surface nanocrystallization (SNC). Tao et al. [6] reported the formation of a nanocrystalline structure on the surface of pure iron plate after USP. The average grain size in the nanograined region was found to be as small as 10 nm. It was also noted that augmenting the peening duration did not notably impact the grain size but did result in an increase in the thickness of the nanograined layer. The scanning electron microscopy (SEM) image of the surface of the coarse-grained Fe specimen, depicted in Fig. 5, shows that the grain size of the as-received material ranges between 20-150 µm. Bright-field and dark-field transmission electron microscopy (TEM) images of the surface of the 450-second USP-treated sample, illustrated in Fig. 6, reveal that the application of USP process resulted in the formation of uniform ultrafine equiaxed grains with random crystallographic orientations on the surface of the pure iron plate.

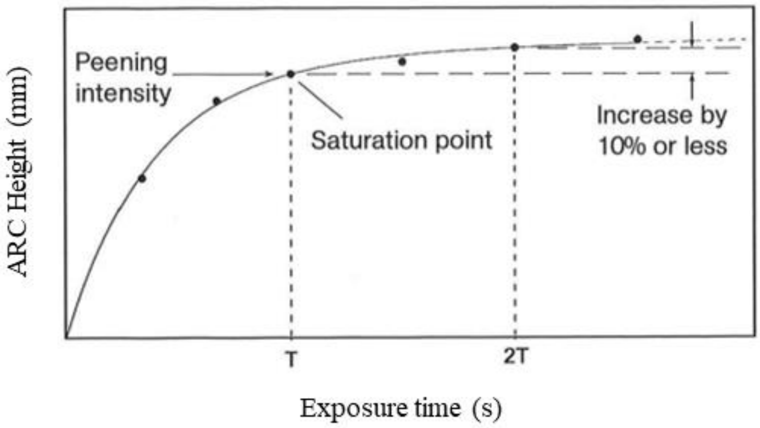

Fig. 3. Variation of arc height with respect to exposure time (saturation curve) [2].

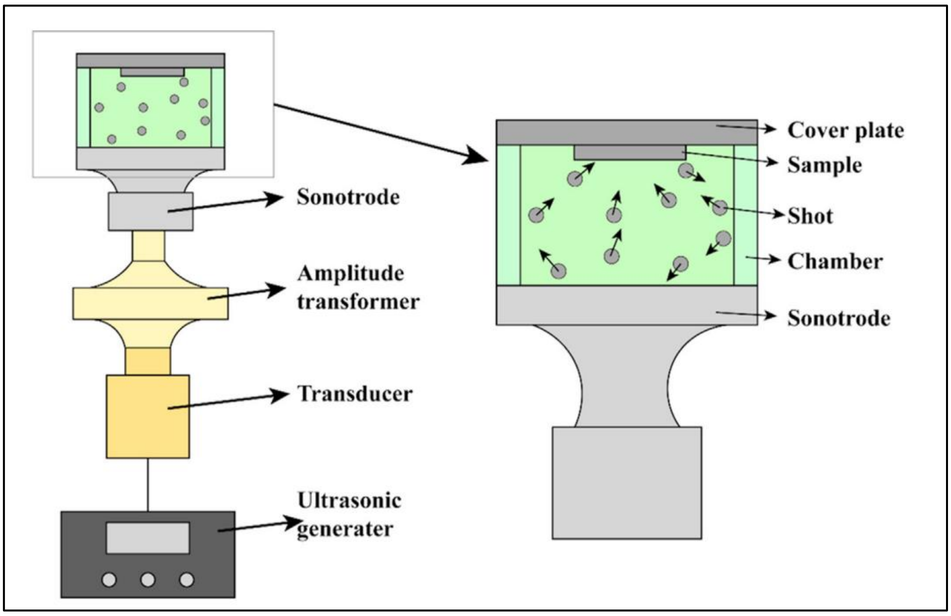

Fig. 4. Schematic of USP process and its components [26].

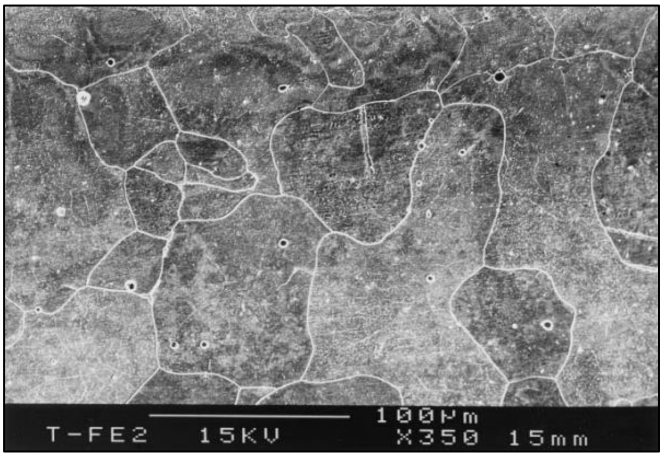

Fig. 5. SEM image of the surface of the as-received Fe sample [6].

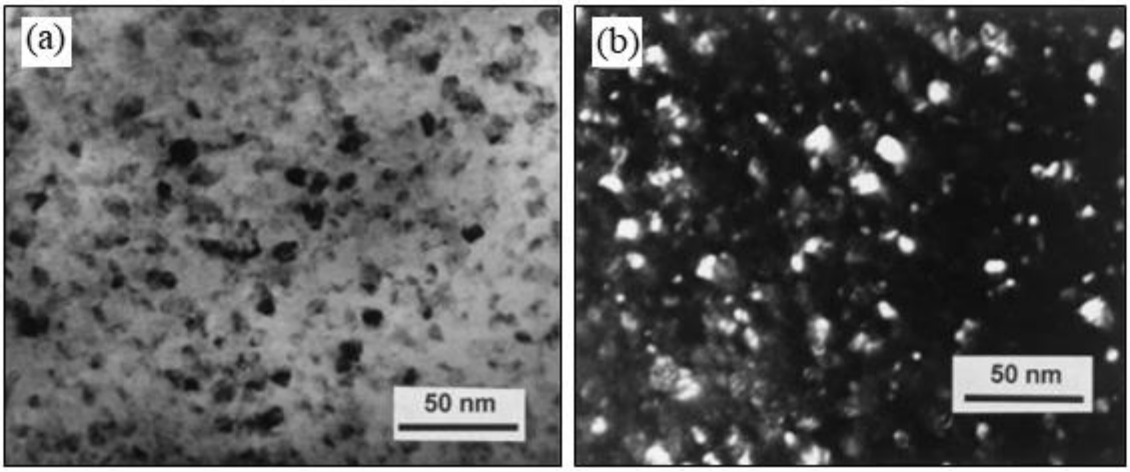

Fig. 6. (a) Bright-field and (b) dark-field TEM images of the surface of the 450-second USP-treated Fe specimen [6].

Liu et al. [7] noted the development of a hardened layer approximately 30 µm thick on the surface of 316L stainless steel subsequent to the application of USP. They observed a nanocrystalline layer around 5 µm thick, comprising grains as small as 10 nm. Beneath this layer, a region with refined grains ranging in size from 10 nm to over 100 nm was formed, extending to a depth of 30 µm. The SEM image of the cross section of the 810-second USP-treated steel sample, shown in Fig. 7, demonstrates that deformations extend approximately 100 µm deep from the surface following the application of USP.

Xing and Lu [8] employed Moire interferometry to quantify the USP-induced residual stresses on the surface and throughout the depth of soft steel. They found that the surface CRS was approximately 309 MPa in magnitude. The distribution of normal stress along the depth of the material is depicted in Fig. 8. Additionally, they discovered the formation of a hardened layer measuring 250 µm in thickness.

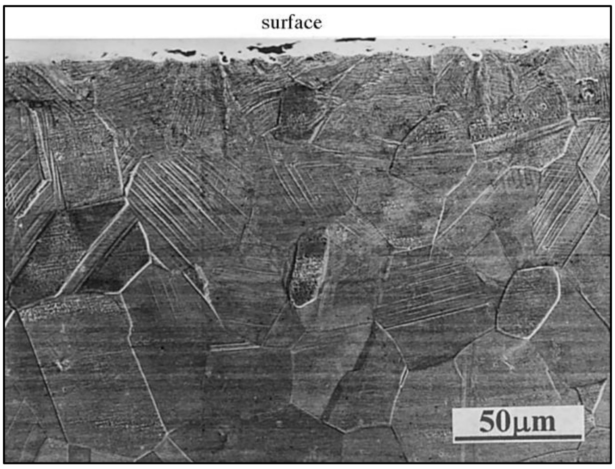

Fig. 7. SEM image of the cross section of 810-second USP-treated steel sample [7].

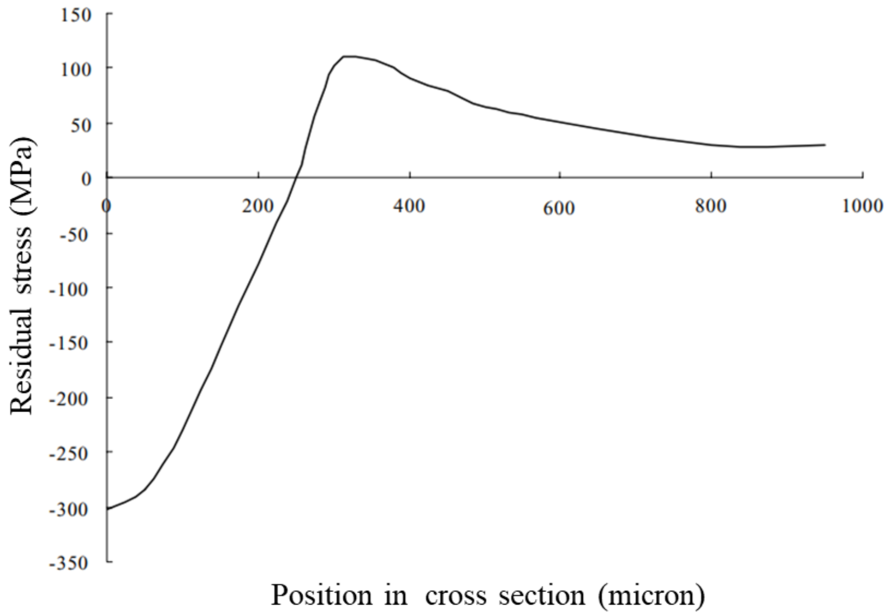

Fig. 8. USP-induced CRS variation along the depth of soft steel [8].

Todaka et al. [9] conducted a comparison between the nanocrystalline surface layer generated in steels by USP and air blast shot peening (ABSP). They outlined a comparison of the general conditions for ABSP and USP processes in Table 1. Their findings revealed that at equivalent coverage levels, the nanocrystalline region created by ABSP is larger than that formed by USP. Moreover, they observed that the deformed structure region is thicker and the strain is smaller in ABSP compared to USP.

Table 1. Process parameters of ABSP and USP [9]

Process type	Shot size (mm)	Shot velocity (mm/s)	Impact direction (degrees)	Coverage rate (%/s)
ABSP	0.05, 0.3	> 100	90	100, 170
USP	0.4	< 20	random	20

Sanda et al. [10] explored the influence of peening duration, shot material, number of shots, and peening distance on the CRS induced on the surface of Inconel 718 by the application of USP. They observed that increasing the peening duration and reducing the peening distance led to an increase in the surface CRS, while increasing the number of shots resulted in a decrease (due to the rise in inelastic collisions and energy losses). Moreover, utilizing WC/Co shots instead of steel shots amplified the surface CRS. Once a certain peening duration was reached, the CRS attained a saturation level, indicating that the system could not induce further plastic deformations on the material. Fig. 9 illustrates the surface state of some USP-treated IN718 samples with respect to peening duration (t), peening distance (H), and shot material.

Yin et al. [11] documented the formation of a 70 µm thick nanograined layer on the surface of pure copper after applying USP with peening duration of 600 s, peening distance of 12 mm, 21 shots of 5 mm diameter, and sonotrode amplitude of vibration of 50 µm.

Zhu et al. [12] observed the formation of a nanocrystalline-amorphous (NC-A) mixed layer upon subjecting pure titanium to USP at room temperature. They investigated the impact of process parameters on the amorphization percentage of the NC-A mixed layer. The process conditions for Zhu's tests are listed in Table 2. They found that the amorphization percentage in the

NC-A mixed layer increased with an increase in peening duration, shot diameter, and sonotrode amplitude of vibration, or with a decrease in the peening distance. The maximum reported amorphization percentage was 44.09%, corresponding to a peening duration of 100 s, shot diameter of 3 mm, sonotrode amplitude of vibration of 40 µm, and a peening distance of 7.5 mm.

Table 2. USP process conditions [12]

Specimen	Peening duration (s)	Shot diameter (mm)	Sonotrode amplitude (µm)	Peening distance (mm)
1	5	2	32	7.5
2	10	2	32	7.5
3	20	2	32	7.5
4	50	2	32	7.5
5	100	2	32	7.5
6	200	2	32	7.5
7	400	2	32	7.5
8	800	2	32	7.5
9	100	1.4	32	7.5
10	100	3	32	7.5
11	100	3	40	7.5
12	100	3	40	10
13	100	3	40	12.5

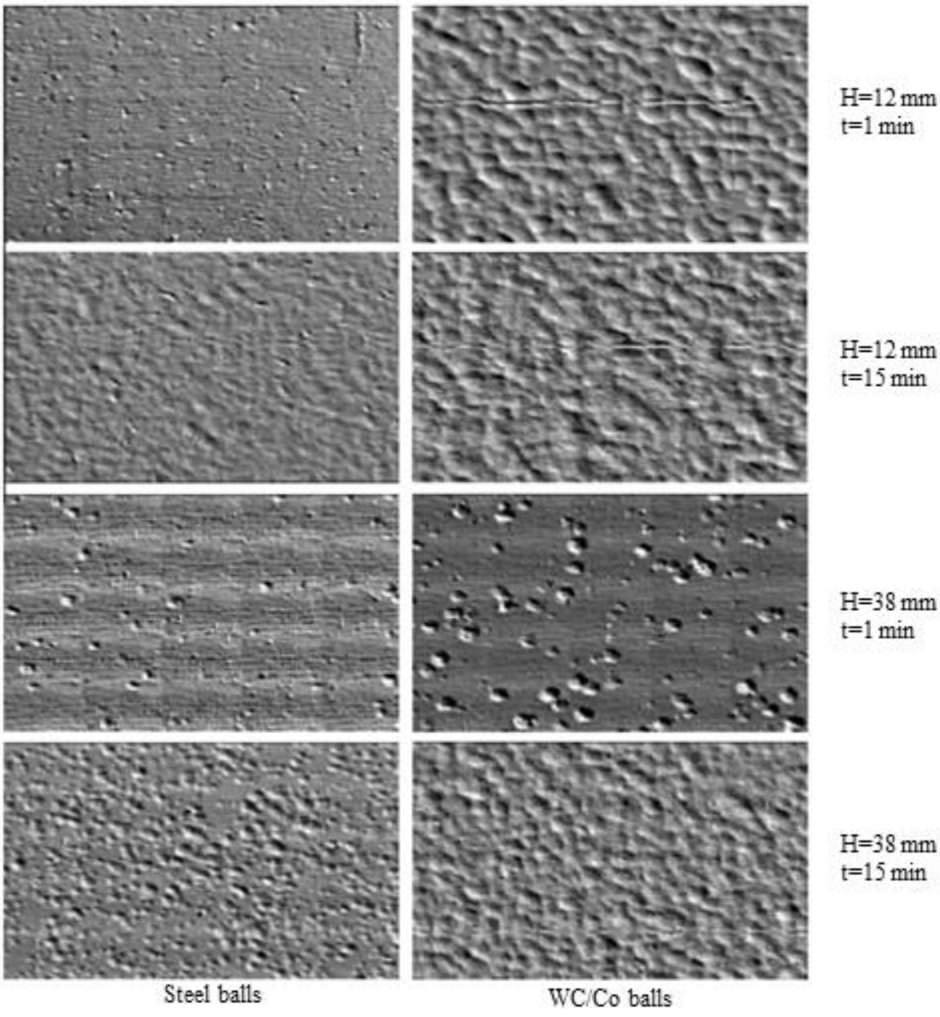

Fig. 9. Surface state of IN718 after USP with different parameters (an extended topograpghy of 3.2 × 2.4 mm area has been measured in each treated sample) [10].

Mahobia et al. [13] examined the influence of peening duration and shot diameter on the grain size of the nanograined region induced on the surface of nickel free high nitrogen austenitic stainless steel by USP. They utilized hardened steel shots with diameters of 2 and 3 mm, along with peening durations of 2 and 8 minutes. Nanograins ranging from 13 to 18 nm were identified on the material's surface. The grain sizes corresponding to different process parameters are summarized in Table 3.

Table 3. Effect of peening time and shot size on nickel free high nitrogen austenitic stainless steel grain size [13]

Peening duration (min)	Shot diameter (mm)	Grain size (nm)
2	2	18
2	3	15
8	2	15
8	3	13

Kumar et al. [14] observed the formation of a nanograined layer on the surface of β titanium following USP with various peening durations. They noted that an increase in the peening duration resulted in reduction of the grain size and an increase in the thickness of the nanograined region.

2.2. Impact of USP on fatigue properties

Surface cracks are a primary cause of fatigue failure, which has been identified as the most prevalent failure mode in materials [17-19]. Research indicates that USP process significantly impacts the fatigue strength of materials. Watanabe et al. [15] investigated the impact of ABSP and USP processes on the fatigue strength of high-strength steel (SNCM439). In the case of USP, two different shot materials, ball bearing (SUJ2) and tungsten carbide (WC) shots, were employed, while other process parameters were held constant. The shots used in ABSP were of rounded cut wire (RCW). According to the results illustrated in Fig. 10, samples treated by both processes exhibited higher fatigue strength compared to the untreated sample. The surface fatigue limit of the specimen treated by USP with WC shots was elevated to 1250 MPa (maximum fatigue limit). Furthermore, the surface fatigue limit of samples treated by ABSP with RCW shots exceeded those USP-

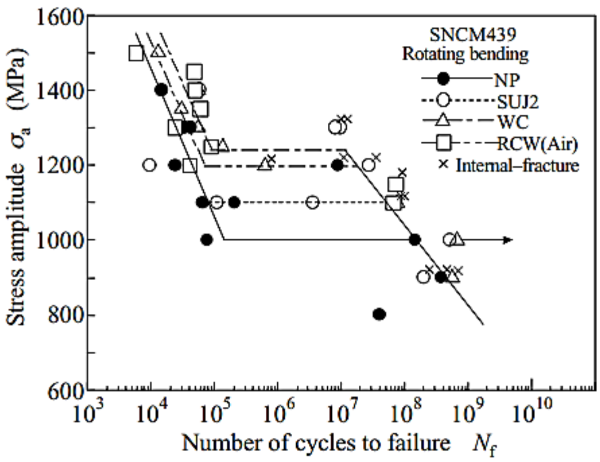

Fig. 10. S-N curves of untreated and treated steel samples [15].

treated by SUJ2 shots.

Pandey et al. [16] examined the impact of the peening duration on the low cycle fatigue (LCF) behavior of 7075 aluminum alloy. Samples underwent USP treatments for durations of 30, 60, 180, and 300 seconds. Processing the sample for 180 seconds enhanced the LCF life of AA7075 due to the combined effect of CRS formation and SNC. However, duration of 300 seconds resulted in the formation of surface cracks and decreased the fatigue life. The effect of USP duration on the number of cycles to failure at different strain amplitudes is depicted in Fig. 11.

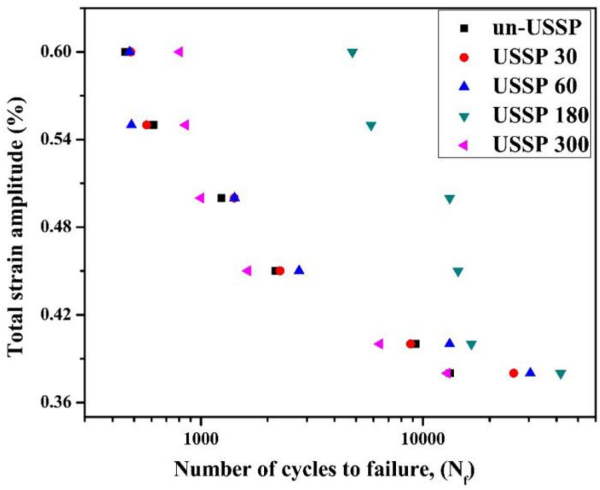

Fig. 11. Effect of USP duration on number of cycles to failure [16].

Kumar et al. [17] found that the LCF life of Ti-6Al-4V was improved by over four times at the lowest strain amplitude following USP with hard steel shots of 3 mm diameter for 5 minutes. The S-N curves of the original and treated samples at various strain amplitudes are depicted in Fig. 12.

Persenot et al. [18] noted that treating Ti-6Al-4V thin struts, constructed via electron beam melting (EBM), with USP using 1 mm 100C6 steel shots and vibration amplitude of 110 µm for 2 hours resulted in a 2.3-fold increase in fatigue strength at 10^5 cycles.

Kumar et al. [19] evaluated the LCF life of high-nitrogen austenitic stainless steel (HNSS) following USP with hard steel shots of 3 mm diameter and vibration amplitude of 80 µm for various peening durations. The fatigue life of the specimens subjected to the corresponding USP conditions is presented in Table 4. It is evident that the LCF life of HNSS was significantly enhanced at low strain amplitudes, while it decreased at higher strain amplitudes. The notable improvement in fatigue life at low strain amplitudes is attributed to the delayed initiation of cracks from the nanograined surface and the associated CRS.

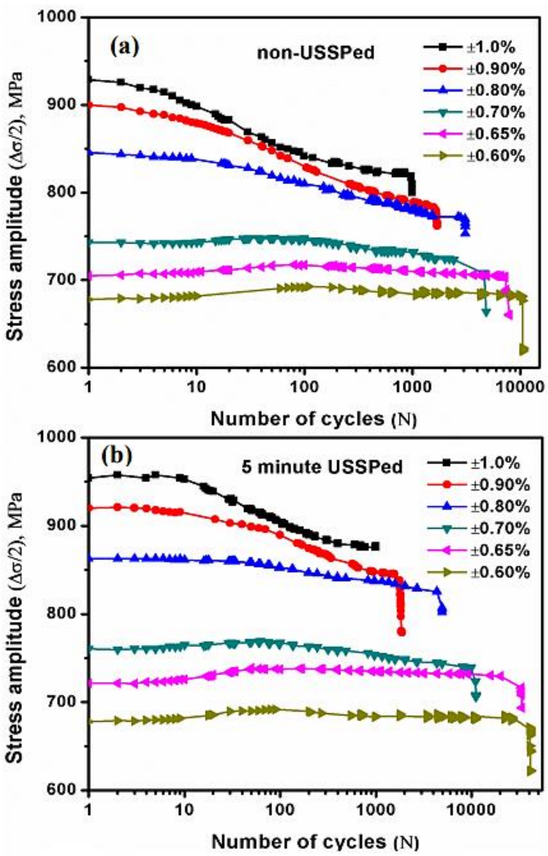

Fig. 12. S-N curves of (a) original and (b) USP-treated samples at different strain amplitudes [17].

Table 4. Effect of peening duration on fatigue life of HNSS [19]

Peening duration (min)	Total strain amplitude ($\pm\Delta\varepsilon_t/2$) (%)	Fatigue life cycles (N_f)
0	0.4	28927
	0.5	15389
	0.6	7330
	0.8	4760
3	0.4	69835
	0.5	28069
	0.6	11834
	0.8	5021
6	0.4	126815
	0.5	28518
	0.6	7629
	0.8	3402
10	0.4	261581
	0.5	20199
	0.6	6841
	0.8	2400
14	0.4	359364
	0.5	17364
	0.6	7038
	0.8	1574
18	0.4	540480

2.3. Influence of USP on surface characteristics, mechanical properties, corrosion behavior, and microstructure of materials

Inducing CRS associated with SNC and enhancing the fatigue strength are not the only effects USP process imparts on materials. Improving surface properties of a material has been shown to be beneficial for enhancing its overall properties [1], which are precisely accomplished by USP. Kumar et al. [20] reported a 3.5% increase in the yield strength, a 2.15% increase in the tensile strength, a 20% increase in the surface hardness, and a 3.4% decrease in the plastic elongation of peak-aged IN718 after USP treatment. The engineering stress-strain curves of IN718 samples with different peening durations are depicted in Fig. 13.

In another study, Kumar et al. [21] discovered that USP enhanced the hot corrosion resistance of Ti-6Al-4V in air and salt environments, as well as salt mixtures, due to SNC. Additionally, Li et al. [22] observed that the surface hardness of 301 stainless steel increased from 275.8±11.7 HV to 522.2±6.9 HV after USP treatment with 1.5 mm shots and the vibration amplitude of 70 µm for 5 minutes. The microhardness variations of the treated and untreated steel samples along the depth are illustrated in Fig. 14.

Pandey et al. [23] conducted USP on AA 7075 using hard steel shots of 3 mm diameter and a vibration amplitude of 80 µm for durations of 15, 30, 60, and 300 seconds. They concluded that the optimum corrosion resistance was achieved with a peening duration of 15 seconds due to higher passivation resulting from SNC, lower plastic deformation, and lower micro strain. Additionally, it was noted that as the peening duration increased, the surface roughness exhibited a steep rise until reaching a certain point, beyond which it increased at a constant rate, as depicted in Fig. 15. This implies that SNC is not the only factor controlling the corrosion resistance, as increased surface roughness can provide active sites for pitting and thereby deteriorate corrosion properties.

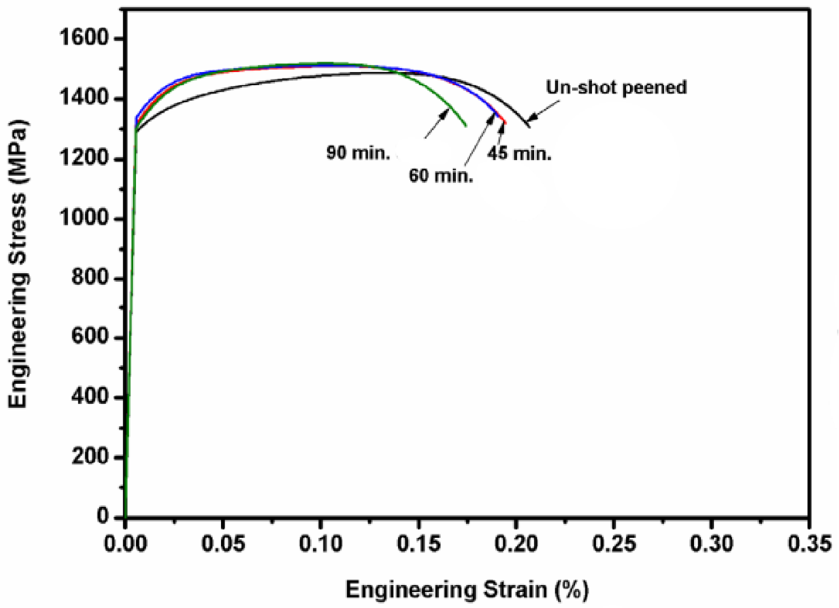

Fig. 13. Tensile properties of peak aged IN718 with respect to different peening durations [20].

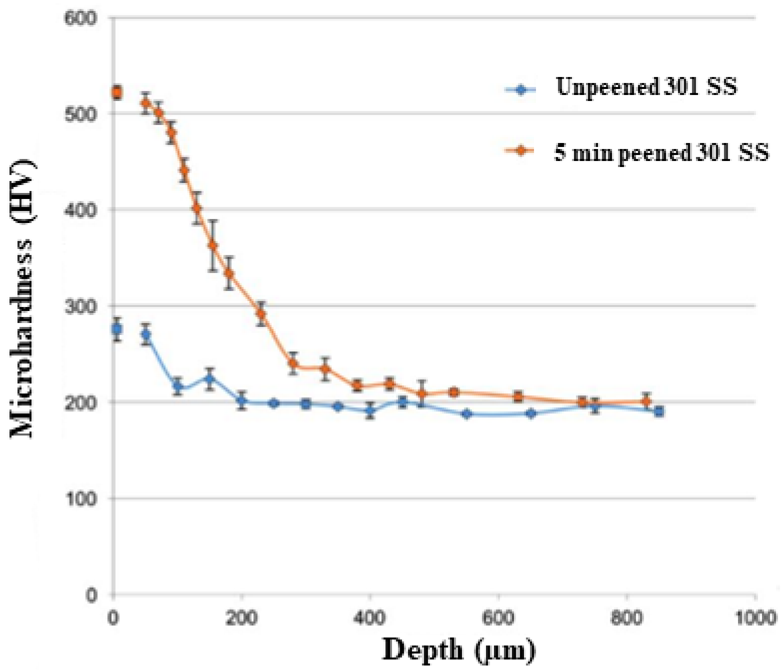

Fig. 14. Microhardness variation of 301 SS samples along the depth [22].

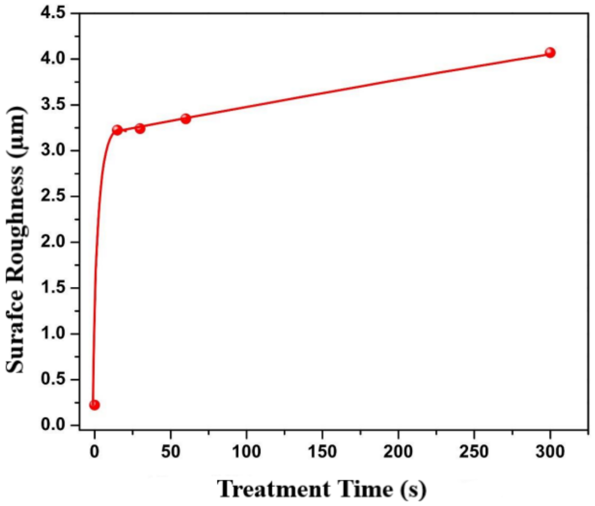

Fig. 15. Effect of peening duration on AA7075 surface roughness [23].

Kumar et al. [24] examined the impact of the shot diameter and the peening duration on the corrosion resistance and microhardness of nitrogen-stabilized stainless steel without nickel, as outlined in Table 5. The variations in the microhardness of samples along the depth are illustrated in Fig. 16. They observed an improvement in the corrosion resistance for samples A2 and B1, while it decreased for longer peening durations due to excessive surface damage.

Table 5. Process parameters [24]

Designation	Shot diameter (mm)	Peening duration (s)
A1	2	30
A2	2	60
A3	2	120
B1	3	30
B2	3	60
B3	3	120

Zhu et al. [25] noted an increase in the surface roughness as the peening duration increased, following the application of USP to WC-8Co samples using 304 standard steel shots with a diameter of 5 mm, whose variation pattern is illustrated in Fig. 17.

Zhang et al. [26] documented a 25% increase in the surface hardness of selective laser melted (SLM) Ti-6Al-4V following USP treatment. They further concluded that increasing the peening duration results in an increase in the CRS both on the surface and in the depth of the samples, as illustrated in Fig. 18.

Kumar et al. [27] noted improved corrosion behavior in all USP-treated Ti-13Nb-13Zr samples compared to the untreated sample. The corrosion rate of the test samples immersed in Ringer's solution for 35 weeks is depicted in Fig. 19.

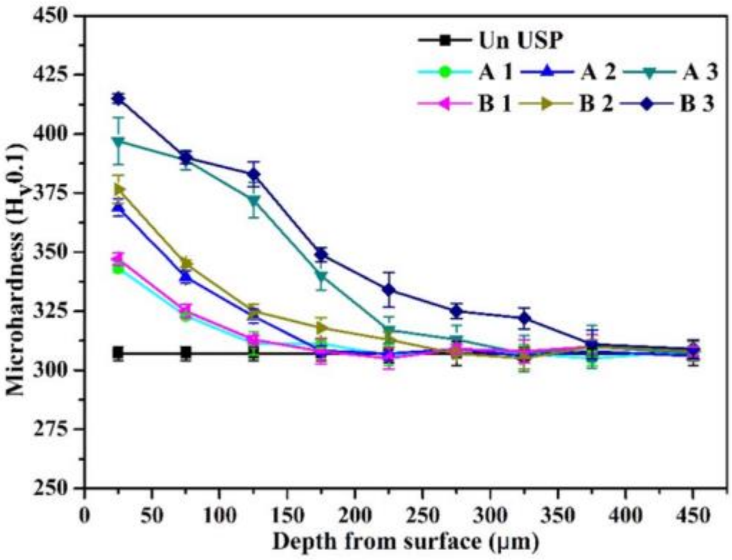

Fig. 16. Microhardness variations along the depth in different samples [24].

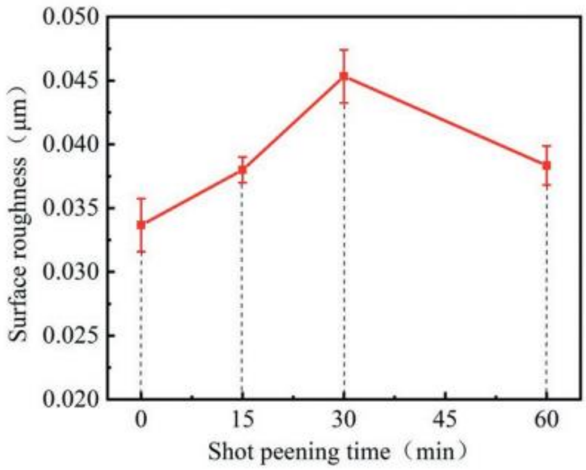

Fig. 17. Effect of peening duration on WC-8Co surface roughness [25].

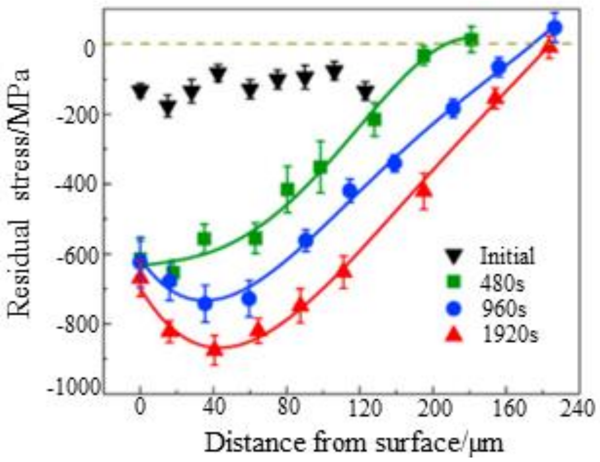

Fig. 18. Effect of peening duration on CRS induced by USP on SLM Ti-6Al-4V [26].

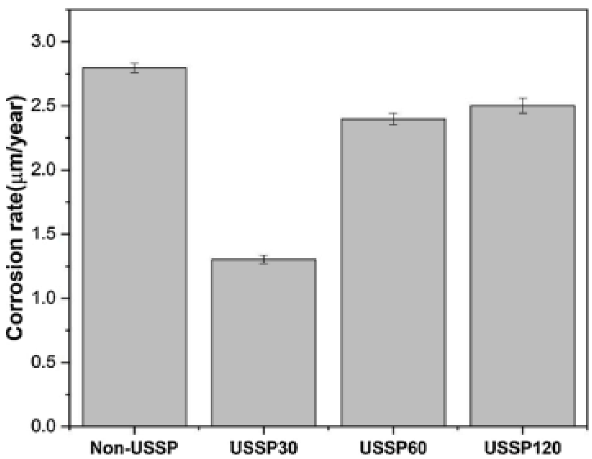

Fig. 19. Effect of peening duration on corrosion rate of Ti-13Nb-13Zr [27].

Chen and Zhang [28] subjected 7A52 aluminum alloy specimens to USP using 304 stainless steel shots with the diameter of 1 mm, the peening distance of 10 mm, and the peening duration of 10 minutes to investigate its impact on the friction and wear characteristics of the material. As depicted in Fig. 20, surface roughness increased after USP treatment. A ball-on-disk friction and wear test was conducted to determine the coefficient of friction and wear rate of specimens under friction loads of 5, 10, 30, and 50 newtons. As illustrated in Fig. 21, both the coefficient of friction and wear rate decreased in USP-treated samples compared to the untreated specimen.

Chen et al. [29] investigated the impact of the peening duration and the peening distance on the surface hardness, yield strength, tensile strength, and elongation of pure copper. After subjecting the sample to USP for 120 seconds, the surface hardness, tensile strength, and yield strength of pure copper increased by 233.5%, 17.1%, and 313.17%, respectively. The variation of tensile properties of pure copper with respect to peening duration is illustrated in Fig. 22.

Xu et al. [30] investigated the impact of the peening intensity on the microhardness, surface roughness, and tensile strength of TC2 thin sheet tensile specimens, as shown in Fig. 23, which were treated with USP on both sides. According to their findings, an increase in the peening intensity led to higher surface roughness, microhardness, and tensile strength. Peening intensities of 0.189, 0.277, and 0.360 mmA resulted in tensile strengths of 772.7, 784.9, and 799.3 MPa, respectively, all of which exceeded the tensile strength of the untreated specimen (752.9 MPa).

Zhang et al. [31] observed a reduction in the coefficient of friction and wear rate of AZ31 magnesium alloy at different sliding speeds following the application of USP to the material. This improvement was attributed to the formation of MgO on material surface, which resulted from SNC. The wear rate of the studied samples under different applied loads and sliding speeds is depicted in Fig. 24.

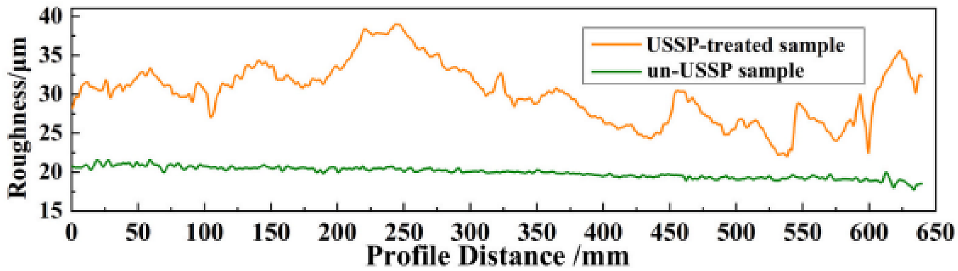

Fig. 20. Effect of USP process on 7A52 surface roughness [28].

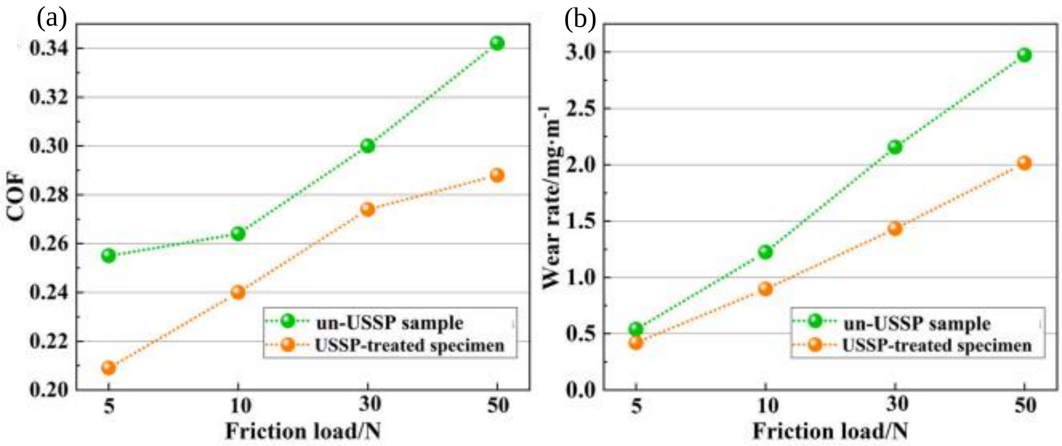

Fig. 21. Effect of USP on coefficient of friction and wear rate of 7A52 [28].

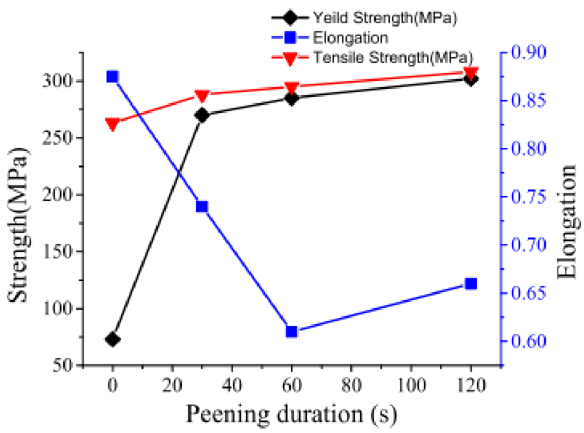

Fig. 22. Effect of peening duration on tensile properties of pure copper [29].

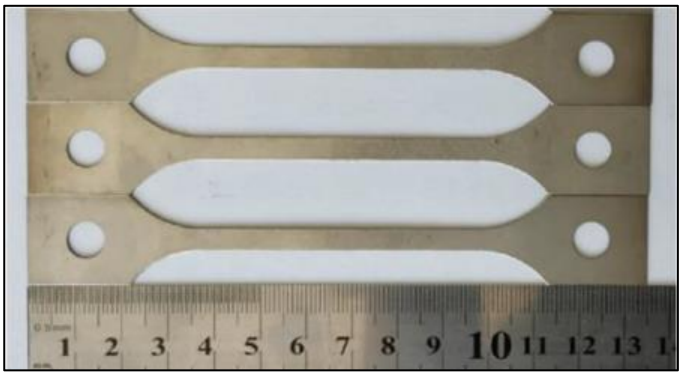

Fig. 23. TC2 tensile specimens [30].

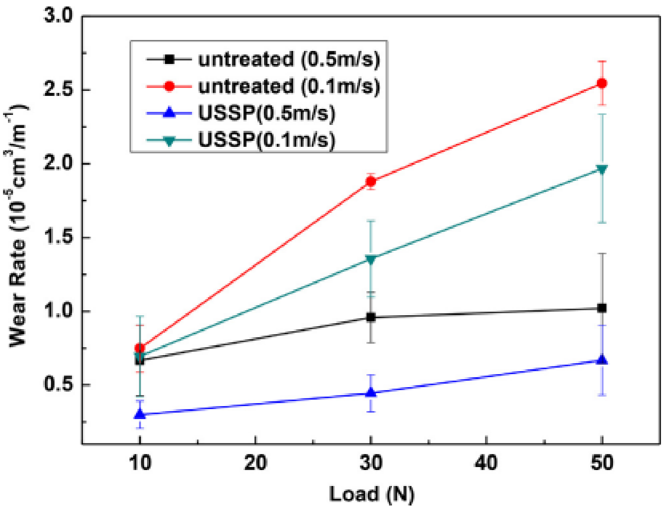

Fig. 24. Effect of USP on wear rate of AZ31 at different sliding speeds [31].

Dong et al. [32] found that USP reduced the wear rate of M50 bearing steel by over 50% under sliding conditions compared to that of the untreated sample. They observed that as the peening duration increased, the wear mechanism tended to shift from oxidative and severe plowing wear to mild plowing wear.

Kong et al. [33] investigated the impact of temperature-assisted ultrasonic shot peening (TA-USP) on mechanical properties of two-phase Mg-Li alloy. The parameters of the experiments are listed in Table 6. Hardness variations with depth of specimens treated with different parameters are illustrated in Fig. 25. Tensile properties of specimens treated with different USP parameters are summarized in Table 7.

Table 6. Process parameters [33]

Sample No.	Peening temperature (ºC)	Peening duration (s)
1	RT	50
2	RT	100
3	RT	200
4	RT	400
5	100	100
6	150	100
7	200	100
8	250	100

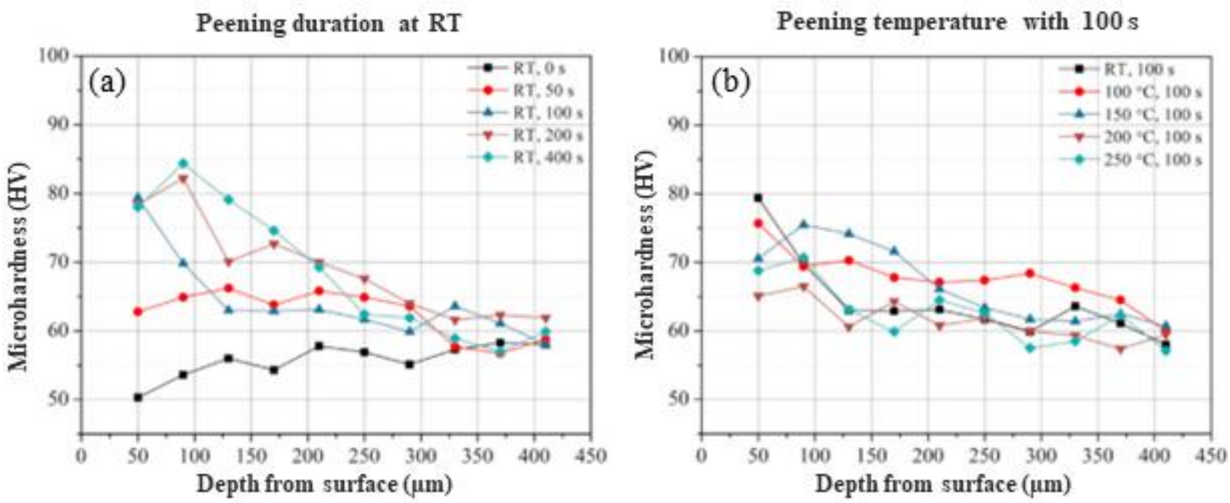

Fig. 25. Effect of peening temperature and duration on microhardness of Mg-Li alloy [33].

Table 7. Effect of temperature and peening time on Mg-Li tensile properties [33]

TA-USP parameters	Tensile strength (MPa)	Yield strength (MPa)	Elongation to failure (%)
RT, 0 s	141.9 ± 8.6	106.2 ± 6.3	29.1 ± 3.8
RT, 100 s	176.5 ± 4.6	152.3 ± 3.4	12.8 ± 2.5
RT, 400 s	172.5 ± 3.9	152.2 ± 4.6	11.5 ± 1.1
100 ºC, 100 s	164.6 ± 0.5	139.7 ± 0.7	10.9 ± 0.3
200 ºC, 100 s	158.3 ± 5.3	134.7 ± 5.4	16.1 ± 1.6

Yin et al. [34] examined the impact of the peening duration on the microhardness and tensile properties of dual phase high entropy alloy (DPHEA), concluding that an increase in the peening duration leads to increased hardness both on the surface and in the depth, as well as higher tensile and yield strength. However, they also noted a decrease in the elongation to failure with increasing the peening duration.

Chen et al. [35] investigated the impact of USP durations of 3, 6, and 9 minutes on the mechanical properties of CrMnFeCoNi high entropy alloy (HEA). They found that the tensile strength increased by 30% to 53%, while the yield strength increased by 129% to 158% compared to untreated samples.

Omidi et al. [36] with the participation of another group of researchers, succeeded in designing, manufacturing and testing the USP setup in Iran for the first time. They conducted a number of experiments based on the full factorial design (FFD), as outlined in Table 8, to investigate the effect of the peening duration and ultrasonic power on the surface hardness of AISI 316L stainless steel. The results revealed that increasing the peening duration and ultrasonic power increased the surface hardness. USP treatment of the specimen at 100 % ultrasonic power for 195 seconds caused the surface hardness to increase from 15.6 HRC to 22.2 HRC. SEM images of the samples “without USP” and “with USP” (No. 4), depicted in Fig. 26, reveal the surface dimples generated by shots impacts.

Table 8. Effect of the peening duration and ultrasonic power on surface hardness of the AISI 316L stainless steel [36]

Sample number	Peening duration (s)	Ultrasonic power (%)	Hardness (HRC)
Without USP	0	0	15.6
1	45	40	17.7
2	195	40	16.8
3	45	100	18.83
4	195	100	22.2

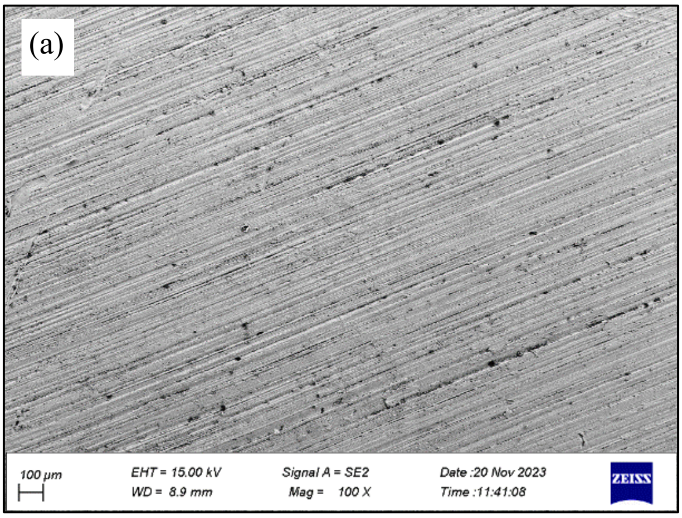

Fig. 26. SEM images of the surface of specimens (a) without USP and (b) with USP (No. 4) [36].

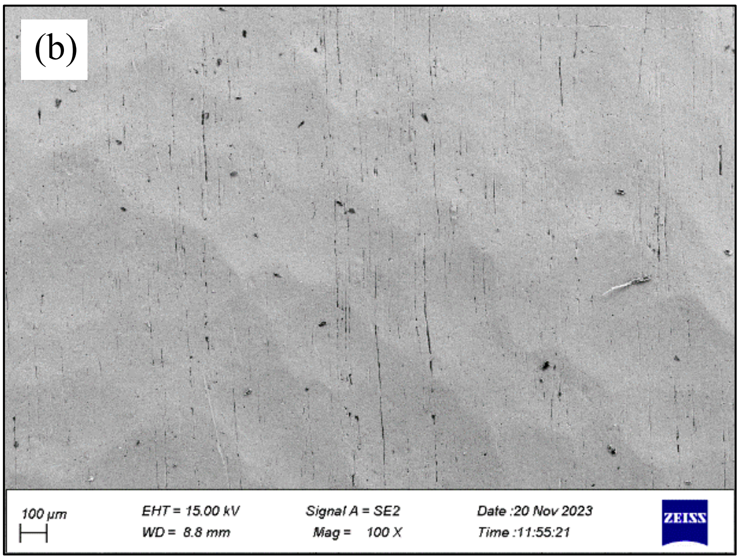

Fig. 26. (*Continued).*

Omidi et al. [37], in another study, investigated the effect of the peening duration and ultrasonic power on the transverse section microhardness of AISI 316L stainless steel samples. The samples were USP-treated in accordance with the experimental conditions outlined in [36]. The transverse section microhardness of cylindrical specimens was measured at depths of 75 and 250 µm using micro-Vickers test equipment, after being cut into halves and cold mounted. Test results are presented in Table 9, revealing that increasing both the peening duration and ultrasonic power increased the microhardness. However, the further from the treated surface, the less the microhardness. In the case of sample No. 1, the microhardness at a depth of 250 µm exceeded the microhardness at a depth of 75 µm, which could be due to the non-uniform flow of the material. In other words, more material accumulated at 250 µm than at 75 µm after the application of USP at 40% ultrasonic power for 45 seconds. The maximum microhardness (346 VHN) was observed at a depth of 75 µm, corresponding to USP treatment of the specimen at a 100% ultrasonic power for 195 seconds.

Table 9. Effect of the peening duration and ultrasonic power on transverse section microhardness of the steel samples [37]

Sample number	Peening duration (s)	Ultrasonic power (%)	Microhardness (VHN)	
			75 µm	250 µm
Without USP	0	0	241.33	241.33
1	45	40	242.33	257
2	195	40	255.33	246
3	45	100	291.66	271.66
4	195	100	346	286

Wang et al. [38] studied the effect of USP on the surface roughness of 2024 aluminum alloy. They used the A-type Almen strip to obtain the saturation curve, as shown in Fig. 27, and to measure the peening intensity in correspondence with the USP parameters listed in Table 10, for the peening durations of 5, 10, 20, 40, and 80 minutes. The saturation time and peening intensity were determined to be 40 minutes and 0.503 mmA, respectively. Subsequently, thin sheets of 1 mm, 2 mm, and 3 mm thickness were USP-treated according to Table 10 and the aforementioned peening durations. Results showed that increasing the peening duration and decreasing the sheet thickness reduced both the arithmetic mean deviation (R_a) and total height of the roughness profile (R_z), as graphically illustrated in Fig. 28.

Table 10. USP parameters for treating 2024 aluminum alloy [38]

Shot material	Shot diameter (mm)	Peening distance (mm)	Amplitude of vibration (µm)	Number of shots	Frequency of vibration (kHz)
SS 304	6	60	40	76	15

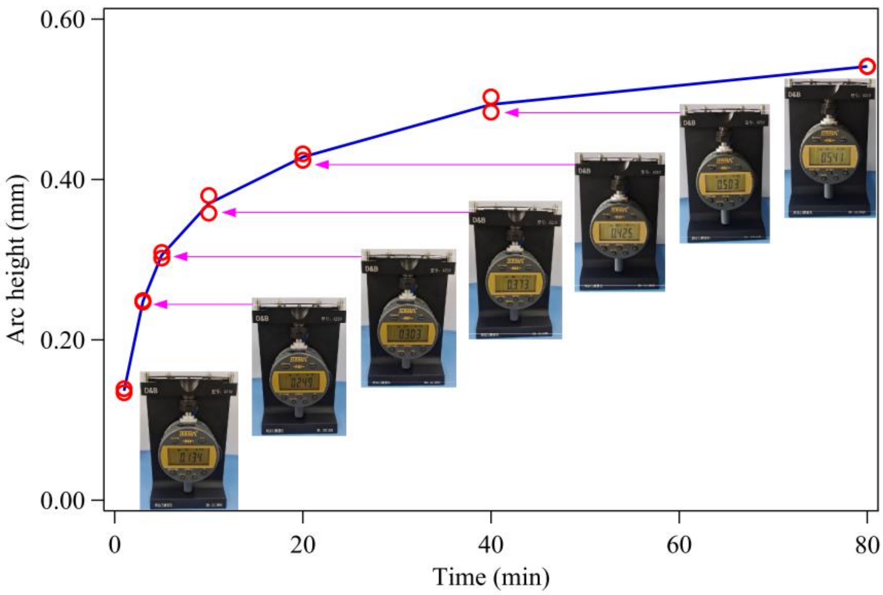

Fig. 27. Arc height variation of A-type Almen strip with respect to peening duration [38].

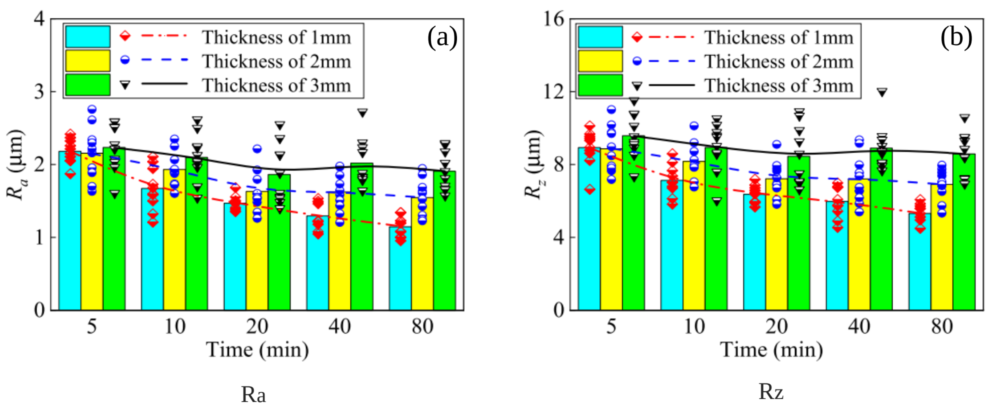

Fig. 28. Effect of peening duration and sheet thickness on (a) arithmetic mean deviation and (b) total height of the roughness profile [38].

Han et al. [39] investigated the effect of USP and USP followed by polishing on the surface roughness and corrosion behavior of AZ80M magnesium alloy. The samples were treated with USP using 3 mm diameter tungsten carbide balls, a peening distance of 15 mm, and vibration amplitude of 50 µm for 4 minutes. The R_a value of the test samples increased from an average of 0.045 µm to 1.165 µm after USP treatment. However, after polishing the USP-treated samples, the surface roughness was restored to an average value of 0.043 µm. The steady-state open circuit potential of the untreated, USP-treated, and "USP + Polishing" specimens in 3.5 wt.% NaCl solution was -1.563 V, -1.583 V, and -1.551 V, respectively. This indicates that the application of USP increased the samples' tendency to corrode due to the increase in surface roughness. In contrast, the polished USP-treated samples showed significantly improved resistance to corrosion, attributed to a more uniform microstructure distribution provided by polishing. Surface morphologies of as-received, USP-treated, and polished USP-treated magnesium samples immersed in 3.5 wt.% NaCl solution for 1, 3, and 24 hours are shown in Fig. 29. The corrosion intensifies by increasing the immersion time. The untreated samples exhibited expanding corrosion likely due to their uneven surface. The USP-treated surface showed the most severe corrosion behavior, while the polished USP-treated sample surface remained relatively consistent, demonstrating the effectiveness of polishing after USP treatment.

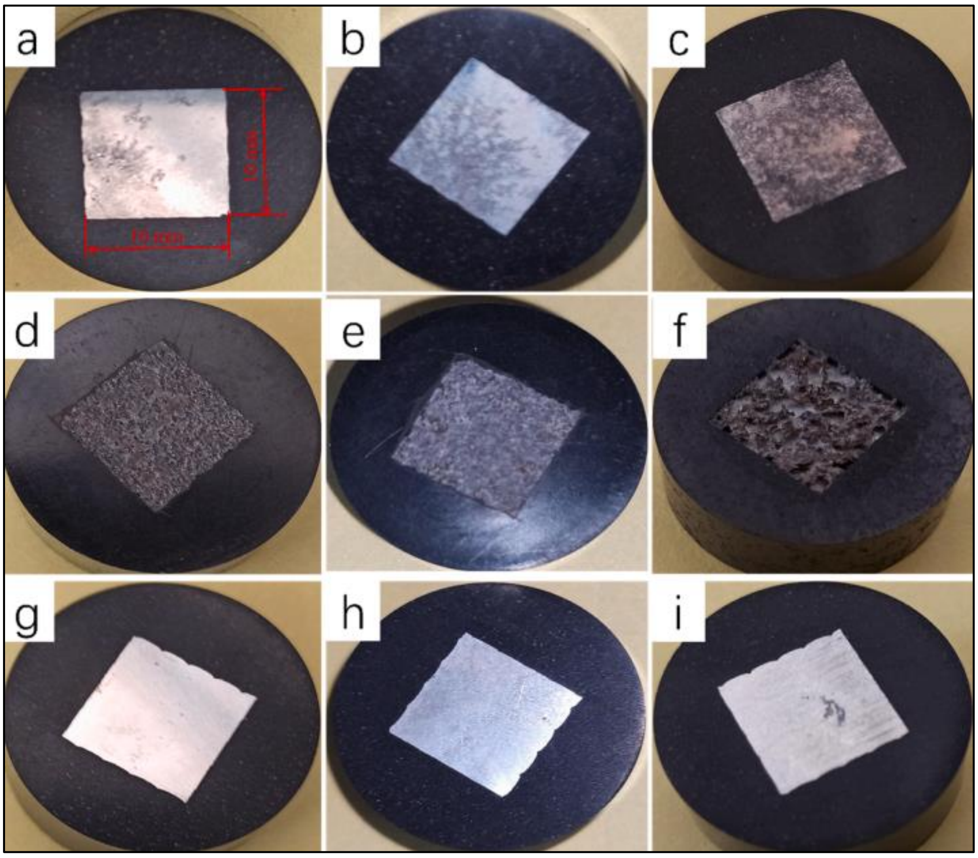

Fig. 29. Surface morphologies of (a, b, c) untreated, (d, e, f) USP-treated and (g, h, i) polished USP-treated samples immersed in 3.5 wt.% solution for 1, 3, and 24 hours (from left to right). Each specimen feature a surface area of (10 × 10) mm^2 [39].

3. Conclusion

Ultrasonic shot peening (USP), a relatively recent surface hardening technique, involves exciting spherical balls (shots) using an ultrasonic vibrating device operating at frequencies above 20 kHz. These oscillations cause the shots to randomly impact the workpiece surface, generating compressive residual stresses (CRS) that refine the material's surface grains. The process boasts a considerable range of controllable parameters, making it straightforward to integrate and implement. This paper aims to provide a comprehensive review of relevant literature published over the past two decades, serving as a comprehensive guide for individuals interested in understanding the USP process and its impact on materials' properties.

Based on the reviewed literature, the following conclusions emerge:

- USP forms a hardened layer on the material's surface, reaching depths of up to 30 µm, with a fraction consisting of a nanograined layer featuring grains as small as 10 nm. The longer the peening duration, the thicker the hardened layer.
- As the peening duration increases, the CRS increases.
- The induced CRS variations follow a consistent pattern along the depth of the treated workpiece. As one moves further from the

treated surface, CRS reaches a maximum negative value before gradually decreasing to zero or aligning with the residual stress of the untreated part of the workpiece. The peening distance has an adverse effect on the CRS magnitude.

- USP improves the fatigue strength, especially at lower strain amplitudes.
- Increasing the peening duration increases the fatigue strength; however, treating the surface of the material for too long brings about excessive plastic deformations and surface cracks that reduces the material's fatigue strength.
- USP increases surface roughness.
- USP has the potential to elevate surface hardness by 20% to 90%.
- USP enhances both yield and tensile strength, while concurrently reducing the elongation to failure.
- Optimizing the peening duration to an ideal value can enhance corrosion resistance. Prolonged peening durations, however, may induce surface cracks and degrade the material's corrosion behavior.
- USP improves wear and friction properties of materials.

Data availability statement

The authors state that the data supporting the results of this research are available in the paper. Also, data sets created during the current study are available from the corresponding author upon reasonable request.

Conflict of Interest

The authors declare that they do not have any conflicts of interest to report about the current study. The authors state that they do not have any financial conflicts of interest or personal relationships that may have affected their work.

Funding

The authors declare that no funds, grants, or other support were received during the preparation of this manuscript.

4. References

[1] Schulze, V. (2006). *Modern mechanical surface treatment: states, stability, effects*. John Wiley & Sons.

[2] Sarabi, B. (2015). *Design of ultrasonic shot peening device.* [Master's Thesis, Polytechnic University of Milan]. POLITesi. https://hdl.handle.net/10589/132760

[3] Vahdati, M., Mahdavinejad, R., & Amini, S. (2017). Investigation of the ultrasonic vibration effect in incremental sheet metal forming process. *Proceedings of the Institution of Mechanical Engineers, Part B: Journal of Engineering Manufacture*, *231*(6), 971-982. https://doi.org/10.1177/0954405415578579

[4] Rakita, M., Wang, M., Han, Q., Liu, Y., & Yin, F. (2013). Ultrasonic shot peening. *International Journal of Computational Materials Science and Surface Engineering*, *5*(3), 189-209. https://doi.org/10.1504/IJCMSSE.2013.056948

[5] Agarwal, K. M., Tyagi, R. K., Chaubey, V. K., & Dixit, A. (2019, November). Comparison of different methods of severe plastic deformation for grain refinement. In *IOP Conference Series: Materials Science and Engineering* (Vol. 691, No. 1, p. 012074). IOP Publishing. https://doi.org/10.1088/1757-899X/691/1/012074

[6] Tao, N. R., Sui, M. L., Lu, J., & Lua, K. (1999). Surface nanocrystallization of iron induced by ultrasonic shot peening. *Nanostructured Materials*, *11*(4), 433-440. https://doi.org/10.1016/S0965-9773(99))00324-4

[7] Liu, G., Lu, J., & Lu, K. (2000). Surface nanocrystallization of 316L stainless steel induced by ultrasonic shot peening. *Materials Science and Engineering: A*, *286*(1), 91-95. https://doi.org/10.1016/S0921-5093/(00)00686-9

[8] Xing, Y. M., & Lu, J. (2004). An experimental study of residual stress induced by ultrasonic shot peening. *Journal of Materials Processing Technology*, *152*(1), 56-61. https://doi.org/10.1016/j.jmatprotec.2004.02.057

[9] Todaka, Y., Umemoto, M., & Tsuchiya, K. (2004). Comparison of nanocrystalline surface layer in steels formed by air blast and ultrasonic shot peening. *Materials Transactions*, *45*(2), 376-379. https://doi.org/10.2320/matertrans.45.376

[10] Sandá, A., Navas, V. G., & Gonzalo, O. (2011). Surface state of inconel 718 ultrasonic shot peened: Effect of processing time, material and quantity of shot balls and distance from radiating surface to sample. *Materials & Design*, *32*(4), 2213-2220.

https://doi.org/10.1016/j.matdes/2010.11.024

[11] Yin, F., Liu, Y., Xu, R., Zhao, K., Partin, A., & Han, Q. (2018). Nanograined surface fabricated on the pure copper by ultrasonic shot peening and an energy-density based criterion for peening intensity quantification. *Journal of Manufacturing Processes*, *32*, 656-663. https://doi.org/10.1016/j.jmapro.2018.04.003

[12] Zhu, L., Guan, Y., Lin, J., Zhai, J., & Xie, Z. (2018). A nanocrystalline-amorphous mixed layer obtained by ultrasonic shot peening on pure titanium at room temperature. *Ultrasonics Sonochemistry*, *47*, 68-74. https://doi.org/10.1016/j.ultsonch.2018.04.017

[13] Mahobia, G. S., Kumar, C. S., & Chattopadhyay, K. (2019). Nanocrystallisation of nickel free high nitrogen austenitic stainless steel through ultrasonic shot peening. In *Key Engineering Materials* (Vol. 813, pp. 43-48). Trans Tech Publications Ltd. https://doi.org/10.4028/www.scientific.net/KEM.813.43

[14] Kumar, P., Mahobia, G. S., & Chattopadhyay, K. (2020). Surface nanocrystallization of β-titanium alloy by ultrasonic shot peening. *Materials Today: Proceedings*, *28*, 486-490. https://doi.org/10.1016/j.matpr.2019.10.174

[15] Watanabe, Y., Hattori, K., Handa, M., Hasegawa, N., Tokaji, K., Ikeda, M., & Duchazeaubeneix, J. M. (2003). Effect of ultrasonic shot peening on fatigue strength of high strength steel. *Shot Peening*, 305-310. https://doi.org/10.1016/j.addma.2019.06.014

[16] Pandey, V., Chattopadhyay, K., Srinivas, N. S., & Singh, V. (2017). Role of ultrasonic shot peening on low cycle fatigue behavior of 7075 aluminium alloy. *International Journal of Fatigue*, *103*, 426-435. https://doi.org/10.3390/met10091262

[17] Kumar, S., Chattopadhyay, K., & Singh, V. (2017). Effect of ultrasonic shot peening on LCF behavior of the Ti–6Al–4V alloy. *Journal of Alloys and Compounds*, *724*, 187-197. https://doi.org/10.1016/j.allcom.2017.07.14

[18] Persenot, T., Burr, A., Plancher, E., Buffière, J. Y., Dendievel, R., & Martin, G. (2019). Effect of ultrasonic shot peening on the surface defects of thin struts built by electron beam melting: Consequences on fatigue resistance. *Additive Manufacturing*, *28*, 821-830. https://doi.org/10.1016/j.addma.2019.06.014

[19] Kumar, C. S., Chattopadhyay, K., Singh, V., & Mahobia, G. S. (2020). Enhancement of low-cycle fatigue life of high-nitrogen austenitic stainless steel at low strain amplitude through ultrasonic shot peening. *Materials Today Communications*, *25*, 101576. https://doi.org/10.1016/j.metcomm.2020.101576

[20] Kumar, S., Rao, G. S., Chattopadhyay, K., Mahobia, G. S., Srinivas, N. S., & Singh, V. (2014). Effect of surface nanostructure on tensile behavior of superalloy IN718. *Materials & Design (1980-2015)*, *62*, 76-82. https://doi.org/10.1016/j.matdes.2014.04.084

[21] Kumar, S., Chattopadhyay, K., Mahobia, G. S., & Singh, V. (2016). Hot corrosion behaviour of Ti–6Al–4V modified by ultrasonic shot peening. *Materials & Design*, *110*, 196-206. https://doi.org/10.106/j.matdes.2016.07.33

[22] Li, K., Spartacus, G., Dong, J., Cao, P., & Shin, K. (2017). Effect of ultrasonic shot peening on microstructure and properties of 301SS. *Materials and Manufacturing Processes*, *32*(16), 1851-1855. https://doi.org/10.1080/10624914.2017.1364863

[23] Pandey, V., Singh, J. K., Chattopadhyay, K., Srinivas, N. S., & Singh, V. (2017). Influence of ultrasonic shot peening on corrosion behavior of 7075 aluminum alloy. *Journal of Alloys and Compounds*, *723*, 826-840. https://doi.org/10.106/j.jallcom.2017.06.310

[24] Kumar, C. S., Mahobia, G. S., Podder, A., Kumar, S., Agrawal, R. K., Chattopadhyay, K., & Singh, V. (2019). Role of ultrasonic shot peening on microstructure, hardness and corrosion resistance of nitrogen stabilised stainless steel without nickel. *Materials Research Express*, *6*(9), 096578. https://doi.org/10.1088/2053-1591/ab2dbe

[25] Zhu, S., Hu, Y., Zhang, X., Zou, Y., Ahmad, T., Zhang, W., Tang, F., & Liang, T. (2020). Experimental investigation on ultrasonic shot peening of WC-Co alloy. *Materials and Manufacturing Processes*, *35*(14), 1576-1583. https://doi.org/10.1088/10426914.2020.1779943

[26] Zhang, Q., Duan, B., Zhang, Z., Wang, J., & Si, C. (2021). Effect of ultrasonic shot peening on microstructure evolution and corrosion resistance of selective laser melted Ti–6Al–4V alloy. *Journal of Materials Research and Technology*, *11*, 1090-1099. https://doi.org/10.1016/j.jmrt.2021.01.091

[27] Kumar, P., Mahobia, G. S., Mandal, S., Singh, V., & Chattopadhyay, K. (2021). Enhanced corrosion resistance of the surface modified Ti-13Nb-13Zr alloy by ultrasonic shot peening. *Corrosion Science*, *189*, 109597. https://doi.org/10.1016/j.corsci.2021.109597

[28] Chen, C., & Zhang, H. (2021). Characteristics of friction and wear of Al-Zn-Mg-Cu alloy after application of ultrasonic shot peening technology. *Surface and Coatings Technology*, *423*, 127615. https://doi.org/10.1016/j.surfcoat.2021.127615

[29] Chen, H., Guan, Y., Zhu, L., Li, Y., Zhai, J., & Lin, J. (2021). Effects of ultrasonic shot peening process parameters on nanocrystalline and mechanical properties of pure copper surface. *Materials Chemistry and Physics*, *259*, 124025. https://doi.org/10.106/j.matchphys.2020.124025

[30] Xu, Q., Cao, Y., Cai, J., Yu, J., & Si, C. (2021). The influence of ultrasonic shot peening on the surface roughness, microstructure, and mechanical properties of TC2 thin-sheet. *Journal of Materials Research and Technology*, *15*, 384-393. https://doi.org/10.1016/j.jmrt.2021.08.029

[31] Zhang, J., Jian, Y., Zhao, X., Meng, D., Pan, F., & Han, Q. (2021). The tribological behavior of a surface-nanocrystallized magnesium alloy AZ31 sheet after ultrasonic shot peening treatment. *Journal of Magnesium and Alloys*, *9*(4), 1187-1200. https://doi.org/10.1016/j.jma.2020.11.012

[32] Dong, Z., Wang, F., Qian, D., Yin, F., Wang, H., Wang, X., Hu, S., & Chi, J. (2022). Enhanced wear resistance of the ultrastrong ultrasonic shot-peened M50 bearing steel with gradient nanograins. *Metals*, *12*(3), 424. https://doi.org/10.3390/met12030424

[33] Kong, M., Zang, T., Wang, Z., Zhu, L., Zheng, H., Gao, S., & Ngwangwa, H. M. (2023). Effects of constrained groove pressing and temperature-assisted ultrasonic shot peening on microstructure and mechanical properties of a two-phase Mg–Li alloy. *Journal of Materials Research and Technology*, *23*, 1947-1967. https://doi.org/10.1016/j.jmrt.2023.01.089

[34] Yin, F., Zhang, X., Chen, F., Hu, S., Ming, K., Zhao, J., Xie, L., Liu, Y., Hua, L., & Wang, J. (2023). Understanding the microstructure refinement and mechanical strengthening of dual-phase high entropy alloy during ultrasonic shot peening. *Materials & Design*, *227*, 111771. https://doi.org/10.1016/j.matdes.2023.111771

[35] Chen, Y., Du, J., Deng, S., Tian, L., & Hu, K. (2023). Effect of ultrasonic shot peening duration on the microstructure and mechanical properties of CrMnFeCoNi high-entropy alloy. *Journal of Alloys and Compounds*, *934*, 168023. https://doi.org/10.1016/j.jallcom.2021.168023

[36] Omidi Hashjin, A., Vahdati, M. & Abedini, R. (2024). *Statistical analysis and optimization of variables affecting the macrohardness of USP-treated samples using the desirability function.* 20th National and 9th International Conference of Manufacturing Engineering (ICME 2024), Tehran, Iran (In Persian).

[37] Omidi Hashjin, A., Vahdati, M. & Abedini, R. (2024). Experimental study and statistical analysis of the effect of ultrasonic shot peening on the microhardness of the cross section of steel samples. *Iranian Journal of Manufacturing Engineering* (In Persian). https://doi.org/10.22034/ijme.2024.470535.1990

[38] Wang, C., Guo, Z., Zhou, B., Li, B., Fei, S., Deng, H., & Shen, G. (2024). Experimental investigation and numerical study on evolution of surface roughness caused by ultrasonic shot peening of 2024 aluminum alloy sheet. *Journal of Materials Research and Technology*. https://doi.org/10.1016/j.jmrt.2024.05.254

[39] Han, M., Du, J., Chen, Y., Sun, Q., & Hu, K. (2024). Influence of ultrasonic shot peening on the microstructure and corrosion behavior of AZ80M magnesium alloy. *Journal of Alloys and Compounds*, *980*, 173633. https://doi.org/10.1016/j.jallcom.2024.173633